# Medium-range order around titanium in a silicate glass studied by neutron diffraction with isotopic substitution

L. Cormier*

*Laboratoire de Minéralogie-Cristallographie, Universités Paris 6 et 7 et IPGP et UMR CNRS 7590, 4 place Jussieu, 75252 Paris Cedex 05, France*

P. H. Gaskell

*Cavendish Laboratory, Madingley Road, Cambridge CB3 0HE, England*

G. Calas

*Laboratoire de Minéralogie-Cristallographie, Universités Paris 6 et 7 et IPGP et UMR CNRS 7590, 4 place Jussieu, 75252 Paris Cedex 05, France*

A. K. Soper

*Rutherford Appleton Laboratory, Chilton, Didcot, OX11 0QX, England*

The structure of a silicate glass of composition $K_2O \cdot TiO_2 \cdot 2SiO_2$ has been reinvestigated by neutron diffraction with isotopic substitution of Ti. These data confirm Ti to be 5-coordinated within a square-based pyramid. The second difference function, which gives directly the Ti-Ti distribution, shows a first Ti-Ti distance at 3.5 Å, with second and third Ti neighbors at 6 Å and 8 Å. These values correspond to a nonhomogeneous distribution of Ti in the glass structure and are consistent with corner-sharing $TiO_5$ pyramids. This explains how this peculiar $TiO_5$ site, with one nonbridging O at 1.68 Å and four O at 1.96 Å, allows Ti to play both a former and a modifier role in the glass structure. The environment of potassium is consistent with a charge compensating role. The presence of Ti-enriched regions in the glass, which is in agreement with recent reverse Monte Carlo simulations, is favored by the potassium atoms acting as charge compensators around the short titanyl bond. [S0163-1829(98)07038-6]

## I. INTRODUCTION

The nature and extent of medium range order (MRO) in glasses has been recently the subject of numerous studies by EXAFS, neutron diffraction with isotopic substitution and anomalous wide angle x-ray scattering.[1–3] These works have shown that low charge cations are not homogeneously distributed into the glass structure but locally concentrated in channels or ordered domains interlacing with the silicate framework. A pioneering work to investigate the environment around a high charge cation, $Ti^{4+}$, was carried out by Wright *et al.* in a silicate glass by neutron diffraction with isotopic substitution but the medium range organization around titanium was poorly defined.[4] However, recent studies have shown that titanium oxide in alkali silicate glasses has important effects on some thermodynamic properties.[5–7] For instance, the variation of the heat capacity at the glass transition temperature can be 50% higher for the Ti-bearing glasses than for the Ti-free glasses, in relation to an ''excess'' configurational entropy in titanosilicate systems. The $Cp$ anomaly increases with Na or K content and with the depolymerization of the network rising to a maximum at the trisilicate composition ($K_2TiSi_2O_7$). The addition of $TiO_2$ into silicate glasses has also drastic effects on other physical properties like thermal expansion,[8] nucleation rate and viscosity.[9–12] It is thus important to clarify the structural role of Ti in order to understand the influence of this element on the physical properties of these glasses.

In early works, x-ray diffraction was used to study the introduction of $TiO_2$ in alkali silicate glasses (Ref. 13) and the polymerization of the network has been investigated by Raman spectroscopy, but little information has been gained on the medium-range environment around Ti.[12,14] In binary $TiO_2$-$SiO_2$ glasses, Ti is 4-coordinated,[15] but several XAS and x-ray absorption near edge structure (XANES) measurements show that Ti-containing silicate glasses can be considered as composition-dependent mixtures of 4-, 5- and 6-coordinated Ti.[16,17]

The most comprehensive investigation of this system was carried out by Wright *et al.* and Yarker *et al.*[4,18] The Ti site geometry in alkali silicate glasses was determined in a $K_2O$ $TiO_2$ $2SiO_2$ (KTS2) glass by neutron diffraction with isotopic substitution of Ti, combined with extended x-ray absorption fine structure (EXAFS) and XANES measurements on the same glass. This work shows the presence of 5-coordinated Ti, [5]Ti, with approximately one Ti-O distance shorter than the other four. This is consistent with the presence of a *titanyl* group—a square-based pyramid, $TiO_5$—which is observed in crystalline $Na_2TiSiO_5$ in contrast to many other crystalline alkali-titanium silicates, where octahedral coordination of Ti is found. This neutron investigation was pioneering in the sense that differences between the scattered intensity measured for glasses with different Ti isotopes were used to obtain information on the environment around Ti. This includes an estimate of the Ti-Ti correlation function by performing a double difference, which showed a

first Ti-Ti distance at about 3.5 Å and the probability of a second peak at about 6 Å. The reliability of the information was limited by the small range of momentum transfers and a poor signal statistics. In particular, evidence relating to the medium range order is fairly scanty and little or no interpretation of the data beyond first neighbors was attempted. However, an accurate and detailed description of the MRO may be just what is needed to understand the physical properties of this glass.

This paper presents data on the local- and medium-range order around Ti in $K_2O$ $TiO_2$ $2SiO_2$ glass. This composition, which shows a large thermodynamic anomaly at $T_g$, is important because of the need for a firm understanding of the structure at local and medium-range levels around 5-coordinated Ti, $^{[5]}$Ti. Indeed, this glass contains about 85% $^{[5]}$Ti, according to recent XANES measurements, in contrast to many other silicate glasses which contain more complex mixtures of the various Ti coordination states.[16,17] Finally, the results obtained by Yarker *et al.* are sufficiently important to warrant confirmation by state-of-the art measurements. In the present study, information has been obtained on the silicate network and the environment of potassium from the total correlation functions. The first and second difference functions allow a better understanding of the Ti environment at the medium range scale. Ti-Ti distances at 3.5, 6, and 8 Å were obtained from the second difference function, indicating an *inhomogeneous distribution* of Ti in the glass structure and corner-sharing of the $TiO_5$ polyhedra. In combination with reverse Monte Carlo modeling,[24] we show the existence of Ti-rich regions probably associated with potassium atoms, which could act as charge compensators near the short titanyl bond. By contrast to this titanyl oxygen which is not bonded to the silicate network, the four other oxygen ligands are shared with Si and Ti second neighbors by corner linkage between polyhedra.

## II. EXPERIMENTAL

Starting materials were pure, dehydrated, reagent grade $SiO_2$ and $K_2CO_3$. Two titanium oxides enriched (by Eurisotop, Orsay, France) respectively in $^{48}$Ti isotopes (99.22%, the neutron scattering length, $b$, is $-6.00\pm0.03$ fm) and $^{46}$Ti isotopes (73.26%, $b=2.57\pm0.06$ fm) were used. All the $b$ values were calculated using the isotopic composition of each oxide, measured by inductively coupled plasma mass spectrometry (ICP-MS). Three samples of composition $K_2O$ $TiO_2$ $2SiO_2$ were synthesized identical in all respects except for the Ti isotopic composition. One sample was made with the almost pure $^{48}$Ti isotope, another with essentially the $^{46}$Ti isotope and the third is an equal mixture of the two titanium oxides, $^{mix}$Ti. The appropriate quantities were measured by taking into account the various molecular weights of each $TiO_2$ oxide. The powders were pre-heated at 500 °C over 2 hours, then melted in a platinum crucible at 1250 °C for 2 hours. Two cycles of quenching, grinding in an agate mortar and remelting were made to ensure homogeneity. The melts were finally quenched by partial immersion of the crucible in water.

The samples were confirmed to be amorphous by x-ray diffraction. The glass composition and homogeneity was analyzed using the Cameca Microbeam electron microprobe

TABLE I. Composition of the three glasses measured by electron microprobe (atomic%).

| Glass | Si | K | Ti | O | Total |
|---|---|---|---|---|---|
| $^{48}$Ti | 17.15 | 15.32 | 8.35 | 58.91 | 99.73 |
| $^{mix}$Ti | 17.39 | 14.74 | 8.35 | 59.17 | 99.65 |
| $^{46}$Ti | 17.35 | 15.00 | 8.35 | 59.17 | 99.87 |
| Theory | 16.67 | 16.67 | 8.33 | 58.33 | 100 |

at the Universités Paris 6/7 (Table I). The deviations from the nominal composition are caused by volatilization of $K_2O$. The differences between each sample affect directly the accuracy of the difference data. As discussed below, the error is not large—distances and coordination numbers obtained from fits to two difference datasets are very small. The samples are colorless except for the mixed glass which shows a faint brown coloration (also observed by Yarker *et al.* for the $^{46}$Ti)[18] due to a very low contamination of Pt from the crucible. EPR measurements on each sample confirmed that no significant amount of $Ti^{3+}$ is present in the glasses. The density of each sample was determined at the Institut de Physique du Globe (Paris, France) using an Archimedes method with toluene as the liquid reference. The average value of the atomic number density is 0.0645 $\pm0.0001$ atoms Å$^{-3}$.

Neutron total diffraction experiments were carried out on the SANDALS diffractometer at the ISIS spallation neutron source at the Rutherford Appleton Laboratory, U.K. This instrument allows the determination of scattering at low angles (11°–21°) and thus minimizes inelasticity corrections. A wide range of scattering vectors (0.2 Å$^{-1}$<$Q$<50 Å$^{-1}$ at the time of this experiment) can also be obtained. (**Q** is the scattering vector and $Q=|\mathbf{Q}|=4\pi\sin\theta/\lambda$, where $2\theta$ is the scattering angle and $\lambda$ the wavelength of the probing radiation.) A thin-walled vanadium cylinder was filled with about 7 g of each sample. Diffracted intensities were recorded at room temperature for the three specimens in the container, the empty container and a vanadium rod used for absolute normalization. Counting times were approximately 24 h for the $^{48}$Ti and $^{46}$Ti samples and 30 h for the $^{mix}$Ti. The data were corrected for background and container scattering, absorption, multiple scattering and inelasticity effects using the ATLAS suite of programs.[19] The structure factors were Fourier transformed to give the total correlation functions, $G(r)$.

## III. THEORETICAL BACKGROUND

Neutron diffraction intensity is proportional to the structure factor $S(Q)$, whose the Fourier transform in real space gives the reduced total correlation function, $G(r)$:

$$G(r)=\frac{2}{\pi}\int_0^\infty Q[S(Q)-1]\sin(Qr)dQ. \qquad (1)$$

This function is a sum of all the partial pair correlation functions, $g_{\alpha\beta}(r)$, between two types of atom, $\alpha$ and $\beta$:

$$G(r)=4\pi r\rho_0\sum_{\alpha\beta} W_{\alpha\beta}(g_{\alpha\beta}(r)-1), \qquad (2)$$

where $\rho_0$ is the average atomic number density and the weighting factors, $W_{\alpha\beta} = c_\alpha c_\beta b_\alpha b_\beta$, depend both on the atomic fraction, $c$, and the neutron scattering length, $b$. The structure of a solid containing $m$ atomic species is described by $m(m+1)/2$ partial pair correlation functions. Isotopic substitution allows weighted sums of partial correlation functions to be extracted from the $G(r)$ function and to investigate the environment around the isotopically substituted element. The technique consists of measuring the diffraction for specimens, identical apart from the isotopic composition of one element, $M$. By subtracting two total structure factors, it is possible to select only the partial functions involving the element $M$. The first difference signal, $\Delta_{M-\alpha}(Q)$, can then be Fourier transformed to give $G_{M-\alpha}(r)$:

$$G_{M-\alpha}(r) = 2 \sum_{\alpha \neq M} c_\alpha c_M b_\alpha (b_M - b'_M) g_{\alpha M}(r)$$
$$+ c_M^2 (b_M^2 - b_M'^2) g_{MM}(r). \quad (3)$$

This function is similar to the difference calculated with anomalous x-ray diffraction or EXAFS but a wider $Q$-range and better statistics can be realized with neutron—in particular, this method gives a more accurate determination of the coordination numbers, improves the resolution and extends the range of accurate data in $r$-space.

By measuring the neutron diffraction for three samples, two first difference functions can be calculated:

$$\Delta_M(Q) = 2 \sum_{\alpha \neq M} c_\alpha c_M b_\alpha (b_M - b'_M)(S_{\alpha M}(Q) - 1)$$
$$+ c_M^2 (b_M^2 - b_M'^2)(S_{MM}(Q) - 1)$$

$$\Delta'_M(Q) = 2 \sum_{\alpha \neq M} c_\alpha c_M b_\alpha (b'_M - b''_M)(S_{\alpha M}(Q) - 1)$$
$$+ c_M^2 (b_M'^2 - b_M''^2)(S_{MM}(Q) - 1). \quad (4)$$

If the condition $b_M - b'_M = b'_M - b''_M$ is fulfilled, these functions differ only by the second term involving $M$-$M$ correlations and subtraction of these two first difference datasets then eliminates all the terms except that associated with $M$-$M$. We then obtain a second difference signal, $\Delta(\Delta_{M-\alpha}(Q))$:

$$\Delta(\Delta_M(Q)) = \frac{1}{2} c_M^2 (b_M - b''_M)^2 (S_{MM}(Q) - 1). \quad (5)$$

The Fourier transform gives the distribution of $M$ in the compound:

$$G_{MM}(r) = c_M^2 \frac{(b_M - b''_M)^2}{2} g_{MM}(r). \quad (6)$$

The advantage and limitations of the method and the problems associated with the large systematic and random errors in the second difference are discussed elsewhere.[20,2,3]

## IV. RESULTS

### A. Total functions

Interference functions, $Q[S(Q) - 1]$, are shown in Fig. 1 for the three samples. An excellent signal to noise ratio is
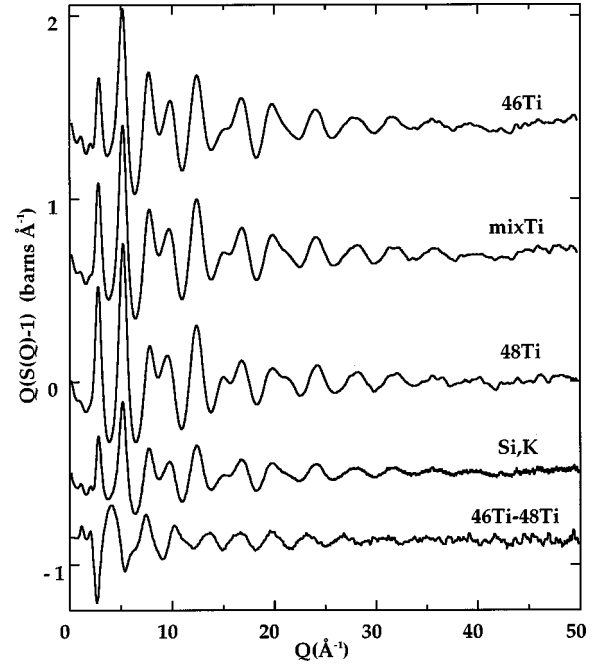


FIG. 1. Interference functions, $Q(S(Q) - 1)$, for the three $K_2OTiO_2 2SiO_2$ glasses ([46]Ti, [48]Ti, and [mix]Ti), the weighted difference (Si, K) and the first difference function between [46]Ti and [48]Ti (some of the curves have been displaced for clarity). The weighted difference (Si, K) has been multiplied by 1.8 to be compared to the total functions (for a similar comparison, the first difference function should be multiplied by 0.3 which would give a weak signal).

obtained up to the highest values of $Q$, which allows good resolution of the data in real space. At high $Q$ values, the structure factors are dominated by correlations at short distances. Oscillations in the range 5–50 Å$^{-1}$ thus indicate well-defined short range order associated with the local structural units of the network. The major changes can be seen in the low $Q$ part ($Q < 5$ Å$^{-1}$) in Fig. 2 and are related to differences in isotopic composition of Ti in each specimen. A first peak at 1.12 Å$^{-1}$ is strongly dependent on the isotopic content: its intensity increases when the Ti neutron scattering length becomes positive. The same behavior oc-
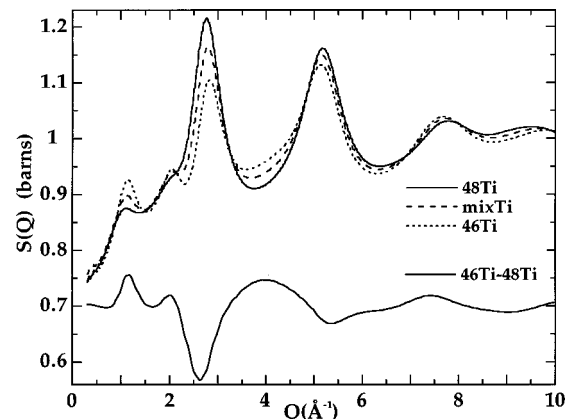


FIG. 2. Total structure factors ([46]Ti, [48]Ti, and [mix]Ti) and differential function ([46]Ti-[48]Ti) in the low-$Q$ region. The variations in the total structure factors are due to differences in the Ti scattering lengths.
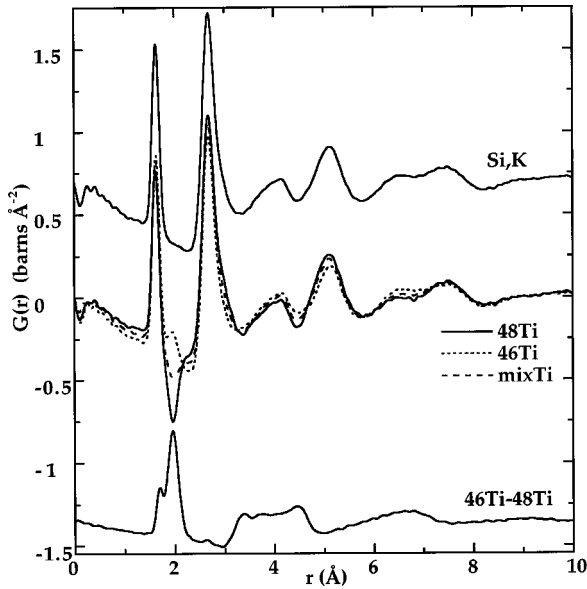
FIG. 3. Fourier transforms of the interference function shown in Fig. 1 (some of the curves have been displaced for clarity). The weighted correlation function (Si, K) has been multiplied by 1.8 to be comparable with the total correlations functions.



FIG. 4. $Q$-space second difference data, proportional to the Ti-Ti partial structure factor.

curs also for the small peak at 2.05 Å$^{-1}$ in contrast to the next two strong peaks in $S(Q)$.

The correlation functions, $G(r)$, obtained by Fourier transformations of $Q[S(Q)-1]$ data with $Q_{max}=45$ Å$^{-1}$, are shown in Fig. 3 for the three samples investigated. To reduce the termination ripples due to the truncation of the $Q$-space data at $Q_{max}$, we multiplied the interference function, $Q[S(Q)-1]$ in Eq. (1) by a Lorch modification function.[21] The slopes at low $r$ are related to the specimen density (slope$=-4\pi r \rho_0 \Sigma W_{\alpha\beta}$) and they agree with the measured density to within 3%. A first peak at 1.62 Å corresponds to Si-O correlations as in crystalline compounds. A peak near 2 Å is positive for the $^{46}$Ti-containing sample and negative for that containing $^{48}$Ti. As $^{48}$Ti has a negative neutron scattering length, the partial correlation functions between $^{48}$Ti and other types of atoms is weighted by a negative factor and thus give rise to a ''negative'' peak in $G(r)$. On the other hand, $^{46}$Ti has a positive $b$ and the $^{46}$Ti$-\alpha$ contribution gives rise to a positive peak. The feature at 2 Å can therefore be assigned to Ti-O correlations. A strong peak at 2.68 Å corresponds to O-O pairs (from the Si and Ti polyhedra) as well as K-O pairs (EXAFS studies on glassy compounds indicate a mean first K-O distance of 2.9 Å).[22]

### B. First difference functions

The first difference function [Eq. (4)], $\Delta_{\text{Ti-}\alpha}(Q)$, obtained by subtracting the total structure factors of $^{48}$Ti and $^{46}$Ti-bearing glasses (Fig. 1, lower curve), has a good signal to noise ratio up to 40 Å$^{-1}$ and is dominated by an oscillation at high $Q$ related to the Ti-O atomic pairs. The Fourier transform of the first difference function, with $Q_{max}=40$ Å$^{-1}$ gives a weighted sum of all Ti-centered pair correlation functions, $G_{\text{Ti-}\alpha}(r)$. This function is dominated by Ti-O correlations ($W_{\text{Ti-O}}$ represents about 65% of contributions to first difference signal). A double peak at 1.68 Å and 1.96 Å vis-

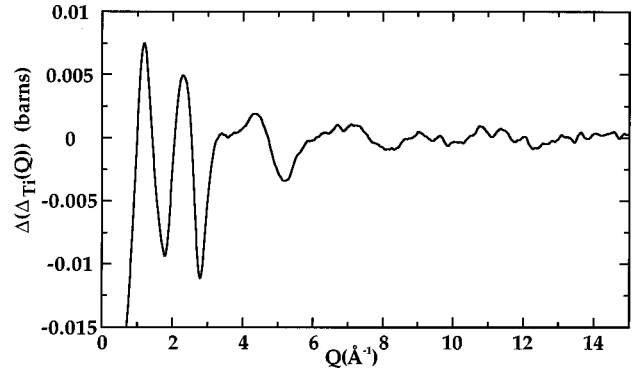ible in Fig. 3 (lower curve) corresponds to two distinct Ti-O distances. A second broad feature between 3 and 4.7 Å can be seen with four bumps that can be assigned to Ti-Si, Ti-K, Ti-Ti and second Ti-O(2) distances, according to crystalline titanosilicates and titanates.

A further difference signal, $\Delta_{\text{Si, K}}(Q)$, can be calculated in which all the Ti-centered terms in the correlation function cancel—except that due to Ti-Ti which is however very small ($<$0.5% of the total signal):

$$\Delta_{\text{Si, K}}(Q) = \frac{1}{b_{46}} {}^{46}S(Q) - \frac{1}{b_{48}} {}^{48}S(Q). \tag{7}$$

In order to compare directly with the total functions, the $\Delta_{\text{Si, K}}(Q)$ function and its Fourier transform (with $Q_{max}=45$ Å$^{-1}$) are divided by a factor $1/(1/b_{46}-1/b_{48})=0.556$ fm$^{-1}$ (Figs. 1 and 3). As we can see in Fig. 3, the Si-O and Ti-O correlations are not well separated; the advantage of the $G_{\text{Si, K}}(r)$ function is that the Si-O peak is completely free from interferences coming from the Ti-O correlations (Fig. 3, upper curve).

### C. Second difference function

The second difference signal, $\Delta(\Delta_{\text{Ti-}\alpha}(Q))$, is obtained by subtracting the first differences, $\Delta_{\text{Ti-}\alpha}(Q)$:

$$\Delta(\Delta_{\text{Ti-}\alpha}(Q)) = {}^{48}S(Q) + {}^{46}S(Q) - 2^{\text{mix}}S(Q). \tag{8}$$

Ideally $\Delta(\Delta_{\text{Ti-}\alpha}(Q))$ is proportional only to the partial structure factor $S_{\text{Ti-Ti}}(Q)$ (see Eq. 5). By using the experimental values, we obtain $\Delta(\Delta_{\text{Ti-}\alpha}(Q))\approx[S_{\text{Ti-Ti}}(Q)-1]/400$. This weak signal contains a considerable level of random noise and is also extremely sensitive to systematic errors associated with composition variations, errors in $b$ values, etc. Measurements of excellent reliability, resolution and signal to noise ratio are therefore essential. The Fourier transform of $\Delta(\Delta_{\text{Ti-}\alpha}(Q))$ gives directly the partial pair distribution function $G_{\text{Ti-Ti}}(r)$ that describes the Ti-Ti distribution in the glass. Due to the degradation of the signal quality at high $Q$ values, we used a $Q_{max}$ value of 10 Å$^{-1}$ to obtain a reasonable resolution. The $Q$- and $r$-space data are shown in Figs. 4 and 5, respectively.

A first peak, due to an incomplete subtraction of the Ti-O correlation, appears in $G_{\text{Ti-Ti}}(r)$ at 2 Å. The three features at 3.5 Å, 6 Å, and 8 Å can be assigned to Ti-Ti atomic pairs. The first agrees with the Ti-Ti peak observed by Yarker *et al.*
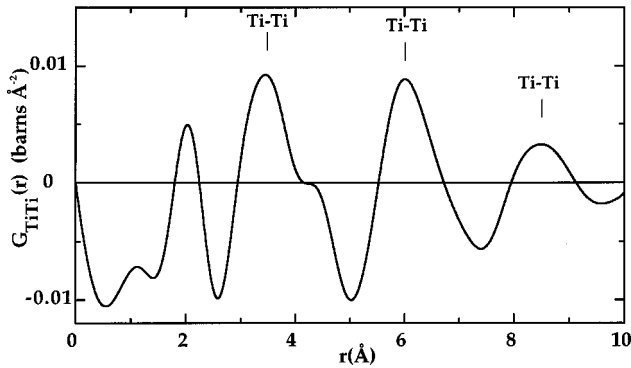
FIG. 5. Fourier transform of the data shown in Fig. 4, giving the distribution of Ti in the glass, $G_{\text{Ti-Ti}}(r)$. The first peak near 2 Å is probably due to a bad subtraction of the Ti-O contribution. The features beyond 2 Å correspond to the Ti-Ti distances.



FIG. 6. Correlation functions for the [46]Ti glass, the weighted difference (Si, K) and the first Ti difference ([46]Ti-[48]Ti). Solid curves represent the experimental data and the dots are the Gaussian fittings using the parameters listed in Tables II and III. These results and the comparison with crystalline references and modeling studies (see text and Ref. 25) allow the main contribution of each peak up to 6 Å to be identified.

but with higher $r$-space resolution associated with the larger range of the $Q$-space data (10 Å$^{-1}$ compared to 7 Å$^{-1}$ for Yarker *et al.*) and an improved statistics of the data.[18] A second peak in the region of 6 Å is also seen in Yarker *et al.*'s data but subject to considerable uncertainty and a third peak at 8 Å is not discernible. The similarity between the two $G_{\text{Ti-Ti}}(r)$ data sets at low $r$ values, obtained from independent diffraction experiments on different specimens, decreases concerns regarding the susceptibility of the second difference method to systematic errors.

### D. Simulation of the total and first difference functions

As no terms involving Ti are contained in the $G_{\text{Si, K}}(r)$ function (we reasonably assumed the Ti-Ti contribution to be negligible), we used this function to obtain information on the silicate network and the environment of potassium. A series of Gaussian functions up to 3.5 Å was used to determine the interatomic distances, $r$, the coordination numbers, $N$, and the standard deviations, $\sigma$. The Gaussians were convoluted with a peak shape function corresponding to the cosine transform of the Lorch function used to smoothly truncate the $Q$-space data. Fits are shown in Fig. 6 (upper and middle curves) and the fitting parameters are listed in Table II.

The first peak corresponds to the 4.0 O neighbors around tetrahedral Si, with a Si-O distance of $1.623 \pm 0.002$ Å. The peak at 2.7 Å was simulated with contributions from the O-O and K-O correlations, using the mean K-O distance of 2.9 Å reported in glasses using EXAFS.[22] This value was fixed: other parameters for the K-O and O-O contributions were allowed to vary. The coordination number of 7.8 found for K is close to values of 8–9 observed by EXAFS in K-containing silicate glasses.[22] A Si-Si correlation at about 2.9 Å should also be included in the high-$r$ part of the peak at 2.7 Å but, due to its small weighting factor, this correlation does not give a significant contribution.

The Ti-O atomic pair was fitted with two Gaussians in the first difference function, $G_{\text{Ti-}\alpha}$, (Fig. 6, lower curve). As the first Ti-O peak at 1.68 Å coincides with the strong Si-O peak in the total correlation function, it is important to ensure that this contribution is completely removed in the first difference. The total correlation function, $G(r)$, was then fitted up to 2.5 Å with three Gaussian functions: two constructed us-
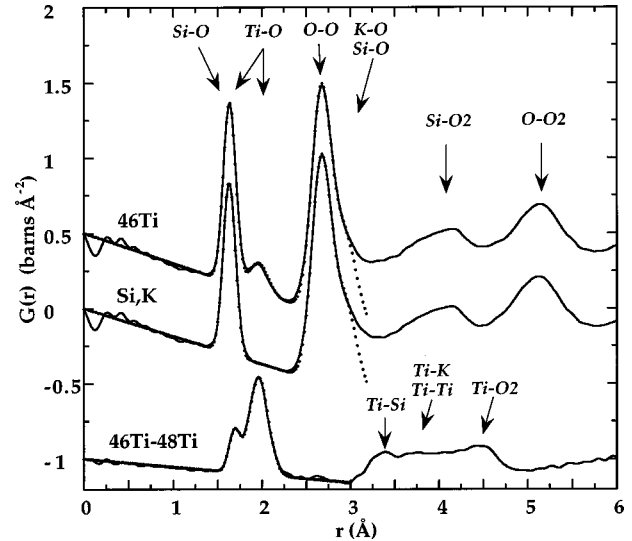
ing the values obtained by fitting the Ti-O correlation in $G_{\text{Ti-}\alpha}(r)$, and the parameters of the third, Si-O Gaussian allowed to float. After fitting, the values for the last Gaussian correspond to the fitting parameters for Si-O obtained from $G_{\text{Si, K}}(r)$. This result demonstrates that the Si-O correlation is negligible in $G_{\text{Ti-}\alpha}(r)$ and the peak at 1.68 Å may be completely attributable to the Ti-O correlation. Additional confirmation comes from the fact that the two first difference functions, $G_{\text{Ti-}\alpha}(r)$, were fitted independently, and the two sets of parameters thus derived agree to within the uncertainties quoted in Table III.

The fitted parameters listed in Table III correspond to a fivefold coordination of Ti in a square-based pyramid with four O at 1.96 Å and one O at a shorter Ti-O distance of 1.68 Å. These results are consistent with previous neutron diffraction (Ref. 18) and EXAFS experiments.[16] However, the two nearest Ti-O distances are not resolved in EXAFS, due to the smaller $Q$-space available.

As the Ti-O distance for [4]Ti is 1.81 Å, a contribution from TiO$_4$ sites will lie between the two peaks at 1.68 and 1.96 Å in $G_{\text{Ti-}\alpha}(r)$. Neutron diffraction data are thus very sensitive to the possible presence of [4]Ti. Though the simulations shown in Fig. 6 do not require a contribution of [4]Ti, we tested the possibility of minor amounts of [4]Ti in $G_{\text{Ti-}\alpha}(r)$. Above 15% of [[4]]Ti, the agreement with experi-

TABLE II. Fitting parameters obtained for simulation of the $G_{\text{Si, K}}(r)$ function (fits of the three total correlation functions give values ranging in the errors given in the table).

|               | Si-O            | O-Si         | O-O          | K-O          |
|---------------|-----------------|--------------|--------------|--------------|
| $r$ (Å)       | $1.623 \pm 0.002$ |              | $2.66 \pm 0.01$ | 2.9          |
| $N$           | $3.98 \pm 0.01$   | $1.12 \pm 0.01$ | $4.9 \pm 0.1$   | $7.8 \pm 0.2$   |
| $\sigma$(Å)   | $0.058 \pm 0.02$  |              | $0.10 \pm 0.1$  | $0.14 \pm 0.1$  |

TABLE III. Fitting values obtained for the double peak in $G_{Ti-\alpha}(r)$ and comparison with previous studies.

| | Present study neutron | Yarker neutron | Yarker EXAFS | Farges EXAFS |
|---|---|---|---|---|
| $r_1$ (Å) | 1.68±0.01 | 1.65±0.02 | 1.64±0.02 | 1.67±0.03 |
| $N_1$ | 0.85±0.1 | 0.7±0.2 | 1[b] | 1.2±0.3 |
| $\sigma^a$ (Å) | 0.05±0.01 | 0.006±0.02 | 0.04 | 0.10±0.04 |
| $r_2$ (Å) | 1.96±0.01 | 1.95±0.01 | 1.93±0.02 | 1.95±0.02 |
| $N_2$ | 4.0±0.1 | 4.0±0.2 | 4[b] | 3.6±0.5 |
| $\sigma^a$ (Å) | 0.10±0.01 | 0.102±0.01 | 0.044 | 0.032±0.04 |
| $r_{average}$ (Å) | 1.91 | 1.91 | 1.87 | 1.88 |
| $N_{total}$ | 4.85 | 4.7 | 5[b] | 4.8 |

[a]$\Delta\sigma$ for EXAFS.
[b]Fixed values.

mental data becomes poor, especially at high $r$ values, so that 15% of [4]Ti is consistent with the neutron scattered data (Fig. 7). Similar simulations (not presented) ruled out the possibility of significant amount of [6]Ti (TiO$_6$ would give a contribution near 1.96 Å). These results agree with a study of the pre-edge features in x-ray absorption spectra at Ti K-edge which indicated the presence of ≈15% of the total Ti to be four-coordinated in the KTS2 glass and the absence of important amount of six-coordinated Ti.[16]

It is not possible to determine accurately the number of Ti nearest neighbors in $G_{Ti-Ti}(r)$ at 3.5 Å because of the large statistical and systematic errors. A rough estimate suggests a mean coordination number of 2 Ti first neighbors.

The presence of correlations at medium range in the total and difference functions is an important indication of order extending well beyond the first coordination shell. A reverse Monte Carlo (RMC) simulation has been recently presented to account for the various correlations observed, by generating a three-dimensional atomic model of the glass structure.[23] The three total structure factors and the first difference signal were used during the fit and excellent agreement was obtained with the simulated structure factors.
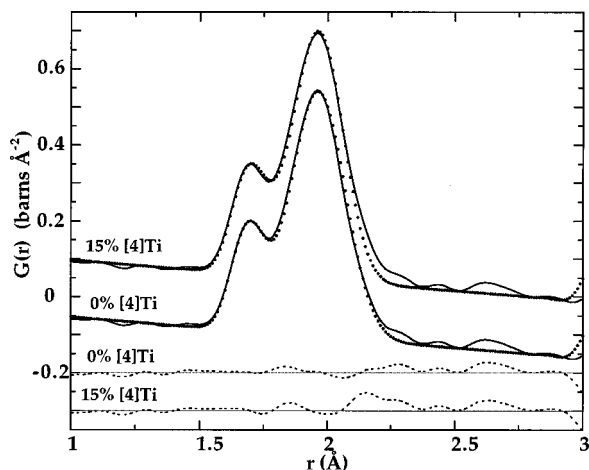


FIG. 7. Simulation of the $G_{Ti-\alpha}(r)$ up to 3 Å by taking into account 0 and 15 of four-coordinated Ti ([4]Ti). The solid curves are the experimental data and the dotted curves are the Gaussian fittings. The two dashed curves represent the difference between the experimental and calculated functions (some curves have been shifted for clarity).

## V. DISCUSSION

### A. Medium range order around Ti

The mean Ti-O distances and coordination numbers found in KTS2 glass are consistent with Ti within a square-based pyramid, with two Ti-O distances at 1.68 Å and 1.96 Å.[18] The existence of titanyl bond is supported by data from Raman spectroscopy of alkali titanosilicate glasses, which show a strong peak at 910 cm$^{-1}$ assigned to a short Ti-O distance.[24] The presence of a minor amount of [4]Ti cannot be ruled out by our neutron diffraction data, but, as pointed out above, more than 15% [4]Ti produces poor simulation of the first double peak in $G_{Ti-\alpha}(r)$. Confirmation that Ti is predominantly [5]Ti, with little or no admixture of [4]Ti, is important since in most silicate glasses a mixture of [4]Ti, [5]Ti, and [6]Ti is observed.[16,17] This justifies the choice of this glass composition to investigate the medium-range order around 5-coordinated Ti. Fivefold coordination has also been seen in other silicate glasses: for example Ni and Fe and, in minor amounts, Si and Al.[22,25]

The first Ti-Ti distance of 3.5 Å corresponds to the distance between titanium in corner-sharing TiO$_5$ pyramids linked by their basal oxygens, an arrangement unknown in crystalline compounds. Titanates show edge-sharing TiO$_5$ pyramids and titanium silicates are based on interlinked corned-shared SiO$_4$ and TiO$_5$ sites, with no direct TiO$_5$-TiO$_5$ linkage. In titanosilicate crystals, two TiO$_5$ units are separated by one or two SiO$_4$ tetrahedra and first Ti-Ti distances are at least 4.6 Å (in natisite, Na$_2$TiSiO$_5$).[26]

Although the accuracy is low, this study suggests that about 2 Ti atoms lie in the second coordination shell. This conflicts with FEFF6 calculations which provide no clear evidence for Ti second neighbors,[16] probably because of the difficulty in distinguishing between Si and Ti which have similar backscattering properties. Similarly, EXAFS measurements indicate 3±1 Si neighbors,[16] the possibility of Ti neighbors being, again, unanswerable. A medium range structure of this kind is supported by RMC modeling of the $S(Q)$ data where 2.4 Ti and 1.8 Si neighbors were found.[23] This indicates that, on average, TiO$_5$ polyhedra are linked to two other TiO$_5$ and two SiO$_4$ polyhedra, contributing to the polymerization of the network. Moreover the simulated Ti-Si distance at 3.26 Å is consistent with corner-sharing SiO$_4$ and TiO$_5$ polyhedra and agrees with the position of the second

peak in EXAFS data.[16] A Ti-Ti distance of 3.5 Å and a Ti-$O_{base}$ distance of 1.96 Å corresponds to Ti-O-Ti angles of 126° which is significantly smaller than the intertetrahedral angle in disilicates. Qualitatively similar information is given by Raman spectroscopy which indicates that Ti cations are incorporated in the silicate sheet-framework structure of disilicate glasses.[12,14]

A random distribution of Ti in a KTS2 glass would give a first Ti-Ti distance of 6.1 Å compared to the measured Ti-Ti distance of 3.5 Å. ($R_{Ti-Ti} = (6 \times 0.63/\pi \rho_0 c_{Ti})^{1/3}$, where $\rho_0$ is the atomic number density and $c_{Ti}$ is the fraction of Ti atoms.) The presence of the short first Ti-Ti distance demonstrates the essential inhomogeneity of the titanium-oxygen ''sublattice,'' which can be visualized by RMC modeling.[23] This inhomogeneous distribution of Ti, a peak at 8 Å in $G_{Ti-Ti}(r)$ (Fig. 5) and the fact that the three Ti-Ti distances are in a recognizable sequence supports the concept of medium range organization of Ti in the glass structure, within domains extending over at least 10 Å. Specifically, if $R_1$ is the first Ti-Ti distance, the second lies near $\sqrt{3}R_1$ and the third near $\sqrt{7}R_1$. Moreover, a distance at $\sqrt{2}R_1$, which is characteristic of an out-of-plane polyhedra linkage, is lacking. As previously proposed for Ca and Ni silicate glasses,[20,27] the presence and the absence of these specific distances can be associated with a two-dimensional ordering of Ti cations at medium range. However, edge sharing polyhedra are generally observed in densely packed domains of low-charge cations such as Ca and Ni,[20,27] rather than corner-shared polyhedra in the Ti-containing glass. This important structural property of Ti in a silicate glass has not been demonstrated before, because spectroscopic methods such as x-ray absorption spectroscopy have a more local character.

In the structure factors presented in Fig. 2, we can observe two small prepeaks at low-$Q$. The first sharp diffraction peak (FSDP) is an important feature in glasses and liquids spectra, as a result of some kind of medium range organization. However, the origin of these FSDP's is still a matter of debate.[28,29] Recently, Gaskell and Wallis (Ref. 29) showed that, in some amorphous solids, the position of these peaks corresponds closely to a strong diffraction peak in a related crystalline phase. The origin of the FSDP could be the existence of ''quasi-Bragg planes'' in the amorphous materials. The position, $Q$, of the FSDP can be related to the lattice spacing, $d$, by the relation $Q = 2\pi/d$ and the width gives an indication on the extent of ordering ($\sim 10$ Å). Two small peaks are present in the total structure factors near 1.12 Å$^{-1}$ and 2.05 Å$^{-1}$, which correspond to distances of 5.6 and 3.1 Å, respectively. The position and intensity of these peaks vary strongly with the Ti isotopic content (Fig. 2). In particular, the variations of intensity are in the opposite direction to those of the following peaks. As the Ti neutron scattering length decreases, the peaks are shifted towards lower values of $Q$ and their intensity decreases. Interpretation is difficult, particularly because no crystalline phase close to the KTS2 composition exists. However, the presence of these peaks in the first and the second difference functions (Figs. 2 and 4) shows that they are associated, at least in part, with Ti ordering. A general feature of all crystalline compounds with [5]Ti-based crystalline compounds is their layer-like structure because of the peculiar asymmetric structure of the $TiO_5$ square-based pyramids. Interplanar separations of about 6 Å

are generally observed. Moreover the simulated neutron diffraction patterns of $Ba_2TiSi_2O_8$ (fresnoite)[30] and $Na_2TiSiO_5$ (natisite)[26] exhibit a peak at respectively 1.05 and 1.38 Å$^{-1}$ which is related to Ti-containing planes.

## B. The peculiar role of potassium

Potassium atoms are located in large 8-coordinated sites with K-O distances of 2.9 Å. These sites are strongly distorted, as shown by the high $\sigma$ value (0.14 Å). A potassium K-edge EXAFS study of aluminosilicate glasses reported similar $\sigma$ values and suggested the environment of K to be more distorted in glasses than in crystals.[31] Smaller K-O distances ($\approx 2.7$ Å) have been obtained in a binary potassium disilicate glass by neutron diffraction,[32] with a smaller $\sigma$ value. Similar values were also determined by x-ray diffraction on potassium silicate glasses.[33] An increase in the K-O distance is observed by EXAFS between silicate glasses (2.8 Å), where K acts as modifiers,[34] and aluminosilicate glasses (3 Å), where K has a charge compensating role near Al sites.[31] This could indicate that potassium atoms play different roles in titanosilicate and silicate glasses.

## C. Structural role of titanium

Ti is well-known to play a dual role in glasses, as former and modifier.[35] This is usually associated with the presence of [4]Ti (network-former) or [6]Ti (network modifier). For Ti in a titanyl group, the two types of oxygen in the pyramidal sites of Ti exert similar influences.[16] The four oxygens at 1.96 Å contribute to the polymerization of the network, each oxygen being linked with one $SiO_4$ tetrahedron or one $TiO_5$ pyramid, in a bridging structural position. On the contrary, the ''titanyl'' (Ti=O) oxygen at 1.68 Å is nonbridging and underbonded. The charge compensation can be satisfied by 3–4 potassium atoms bonded to this oxygen. The much higher solubility of $TiO_2$ in potassic melts than in calcic melts, has suggested a strong interaction between K and Ti components in silicate glasses.[24] The features around 3–5 Å in $G_{Ti-\alpha}(r)$ are compatible with the presence of K atoms around Ti as confirmed by RMC modeling where first Ti-K distances are found between 3.2–4 Å.[23] K-Ti distances of 3.4 Å are also compatible with multiple scattering calculations of the Ti XANES spectra.[16] Furthermore the partial molar volume of $TiO_2$ in KTS glasses is higher than that observed in rutile where Ti is sixfold coordinated, which thus indicates a lower coordination of Ti in KTS glasses. As this partial molar volume increases from Li to K then decreases from K to Cs or for divalent cations,[11,36] potassium atoms are among the best modifiers for charge compensating the ''nonbridging'' oxygen existing in presence of [5]Ti. Most crystals containing [5]Ti are also potassic silicates or titanates.

As the Ti-O-Ti Raman active mode has been observed in alkali silicate glasses with low $TiO_2$ content, the Ti-rich regions evidenced by neutron scattering may also appear at low $TiO_2$ contents.[12,14] The origin of these Ti-rich regions could result from an optimized sharing of the compensating K atoms between Ti sites. Indeed, in $TiO_2$-$SiO_2$ glasses where Ti is found in tetrahedral sites, Raman spectra indicate that a majority of Ti is randomly distributed at low $TiO_2$ content,[37] which is confirmed by the lack of a second neigh-

bors shell in EXAFS spectra.[15] This indicates a more homogeneous distribution of $^{[4]}Ti$ in the glass structure.

The bidimensional character of the Ti-rich regions and the strong association between Ti and K atoms may stabilize Ti in KTS2 glass and explain its weak tendency to crystallize.[7] The same behavior is observed for the titanosilicate glass containing sodium (NTS2), with a similar environment for Ti.[16] This is in contrast with other glass compositions that contain high field strength cations, such as cordierite ($Mg_2Al_4Si_5O_{18}$) or $\beta$-spodumene ($LiAlSi_2O_6$).[9,10] In these glasses, Ti is widely used as nucleating agent to form glass-ceramics.[38] This difference can be explained by a different medium range ordering due to a less stable association between Ti and the compensating cations than in the KTS2 glass, as suggested by Raman spectroscopy.[24]

A coordination change in the Ti site at high $T$ seems to be ruled out as a possible explanation for the origin of the thermodynamic anomaly at Tg, according to recent EXAFS data on Ti-bearing melts.[39] Structural modifications at medium range scale around Ti are more likely. They could result from a disordering or a disruption of the K-Ti association. Further study is in progress in this direction.

## VI. CONCLUSIONS

Neutron diffraction with isotopic substitution of Ti have provided good first and second difference data and these measurements have proved very useful in investigations of the structure of a $K_2OTiO_22SiO_2$ glass. The correlation functions ($G(r)$, $G_{Ti-\alpha}(r)$, and $G_{Ti-Ti}(r)$) show oscillations up to 10 Å which clearly indicate medium range ordering beyond the first coordination shell. The difference technique allows the resolution of the two Ti-O distances: four O at 1.96 Å and one ''non-bridging'' O at 1.68 Å, corresponding to a square-based pyramid for the Ti site. Moreover the neutron diffraction data suggest only minor amounts of $^{[4]}Ti$ and $^{[6]}Ti$ sites.

The medium range structure around $^{[5]}Ti$ has been extensively studied with the second difference function and reverse Monte Carlo simulations.[23] The second difference data show a first Ti-Ti distance at 3.5 Å, indicating an inhomogeneous distribution of Ti in the glass, as can be observed in a reverse Monte Carlo simulation.[23] This distance corresponds to corner-sharing $TiO_5$ and $SiO_4$ polyhedra. Potassium atoms are likely to be associated with Ti sites to ensure charge compensation of the short non-bridging titanyl bond. Second and third Ti-Ti distances suggest the presence of extended bidimensional Ti-rich regions. The low-$Q$ features in the structure factors were found to be dependent on the scattering length of the Ti isotope involved. The presence of these peaks in the first and second difference indicates that these structures are dependent on the Ti-Ti distribution.

*Corresponding author. FAX: +33-1 44 27 37 85. Electronic address: cormier@lmcp.jussieu.fr

[1] G. N. Greaves, J. Non-Cryst. Solids **71**, 203 (1985); S. R. Elliott, Nature (London) **354**, 445 (1991).

[2] P. H. Gaskell, in *Methods in Determination of Partial Structure Factors of Disordered Matter by Neutron and Anomalous X-ray Diffraction*, edited by J. B. Suck, P. Chieux, D. Raoux, and C. Rielke (World Scientific, Singapore, 1993), p. 34.

[3] L. Cormier, S. Creux, L. Galoisy, G. Calas, and P. H. Gaskell, Chem. Geol. **128**, 77 (1996).

[4] A. C. Wright, C. A. Yarker, P. A. V. Johnson, and F. A. Wedgwood, in *Non-Crystalline Solids*, edited by G. H. Frischat (TransTech, Aedermannsdorf, Switzerland, 1977), p. 118.

[5] P. Richet and Y. Bottinga, Geochim. Cosmochim. Acta **49**, 471 (1985).

[6] R. A. Lange and A. Navrotsky, Geochim. Cosmochim. Acta **57**, 3001 (1993).

[7] M.-A. Bouhifd, Ph.D. thesis, Université Paris 7, 1995.

[8] P. C. Schultz and H. T. Smyth, in *Amorphous Materials*, edited by R. W. Douglas and B. Ellis (Wiley, London, 1970), p. 453.

[9] A. Ramos, M. Gandais, and J. Petiau, J. Phys. C **8**, suppl. 46, 491 (1985).

[10] T. Dumas and J. Petiau, J. Non-Cryst. Solids **81**, 201 (1986).

[11] D. B. Dingwell, Geochim. Cosmochim. Acta **56**, 3403 (1992).

[12] B. O. Mysen, F. R. Ryerson, and D. Virgo, Am. Mineral. **65**, 1150 (1980).

[13] V. R. José and S. Urnes, Phys. Chem. Glasses **13**, 122 (1972); **15**, 158 (1974); R. Guåker, S. Urnes, and V. R. José, *ibid.* **17**, 41 (1976).

[14] T. Furukawa and W. B. White, Phys. Chem. Glasses **20**, 69 (1979).

[15] D. R. Sandstrom, F. W. Lytle, P. S. P. Wei, R. B. Greegor, J. Wong, and P. Schultz, J. Non-Cryst. Solids **41**, 201 (1980); R. B. Greegor, F. W. Lytle, D. R. Sandstrom, J. Wong, and P. Schultz, *ibid.* **55**, 27 (1983).

[16] F. Farges, G. E. Brown, Jr. A. Navrotsky, H. Gan, and J. J. Rehr, Geochim. Cosmochim. Acta **60**, 3039 (1996).

[17] C. W. Ponader, H. Boek, and J. E. Dickinson, Jr. J. Non-Cryst. Solids **201**, 81 (1996).

[18] C. A. Yarker, P. A. V. Johnson, A. C. Wright, J. Wong, R. B. Greegor, F. W. Lytle, and R. N. Sinclair, J. Non-Cryst. Solids **76**, 117 (1986).

[19] A. K. Soper, W. S. Howells, and A. C. Hannon (unpublished).

[20] P. H. Gaskell, M. C. Eckersley, A. C. Barnes, and P. Chieux, Nature (London) **350**, 675 (1991).

[21] E. Lorch, J. Phys. C **2**, 229 (1969).

[22] G. E. Brown, Jr., F. Farges, and G. Calas, Rev. Mineral. **32**, 317 (1995).

[23] L. Cormier, G. Calas, and P. H. Gaskell, J. Phys. C **9**, 10129 (1997).

[24] J. E. Dickinson, Jr. and P. C. Hess, Geochim. Cosmochim. Acta **49**, 2289 (1985).

[25] L. Galoisy and G. Calas, Geochim. Cosmochim. Acta **57**, 3613 (1993); **57**, 3627 (1993).

[26] H. Nyman and M. O'Keefe, Acta Crystallogr., Sect. B: Struct. Crystallogr. Cryst. Chem. **34**, 905 (1978).

[27] P. H. Gaskell, in *Materials Science and Technology*, edited by R. W. Cahn, P. Haasen, and E. J. Kraner (VCH, Weinheim, 1991), Vol. 9, p. 175.

[28] S. R. Elliott, J. Phys.: Condens. Matter **4**, 7661 (1992).

[29] P. H. Gaskell and D. L. Wallis, Phys. Rev. Lett. **76**, 66 (1996).

[30] S. A. Markgraf, A. Halliyal, A. S. Bhalla, and R. E. Newham, Ferroelectrics **62**, 17 (1985).

[31] W. E. Jackson, G. E. Brown, Jr., and C. W. Ponader, J. Non-Cryst. Solids **93**, 311 (1987).

[32] A. C. Hannon, B. Vessal, and J. M. Parker, J. Non-Cryst. Solids **150**, 97 (1992).

[33] Y. Waseda and H. Suito, Trans. Iron Steel Inst. Jpn. **17**, 82 (1977).

[34] G. N. Greaves, S. J. Gurman, C. R. A. Catlow, A. V. Chadwick, S. Houde-Walter, C. M. B. Henderson, and B. R. Dobson, Philos. Mag. A **64**, 1059 (1991).

[35] B. V. J. Rao, Phys. Chem. Glasses **4**, 22 (1963).

[36] R. A. Lange and I. S. E. Carmichael, Geochim. Cosmochim. Acta **51**, 2931 (1987).

[37] B. O. Mysen, F. R. Ryerson, and V. Virgo, Am. Mineral. **65**, 1150 (1980).

[38] *Glasses and Glass-Ceramics*, edited by M. H. Lewis (Chapman and Hall, London, 1989).

[39] F. Farges, G. E. Brown, Jr., A. Navrotsky, H. Gan, and J. J. Rehr, Geochim. Cosmochim. Acta **60**, 3055 (1996); F. Farges, G. E. Brown, Jr., and J. J. Rehr, Phys. Rev. B **56**, 1809 (1997).